Editors' Suggestion

Hyperuniform Interfaces in Nonequilibrium Phase Coexistence

Raphaël Maire,[1] Leonardo Galliano,[2,3] Andrea Plati,[1] and Ludovic Berthier[3]
[1]*Université Paris-Saclay, CNRS, Laboratoire de Physique des Solides, 91405 Orsay, France*
[2]*Dipartimento di Fisica, Università di Trieste, Strada Costiera 11, 34151, Trieste, Italy*
[3]*Gulliver, CNRS UMR 7083, ESPCI Paris, PSL Research University, 75005 Paris, France*

(Received 1 August 2025; accepted 30 October 2025; published 26 November 2025)

We show that long-wavelength interfacial fluctuations are strongly suppressed in nonequilibrium phase coexistence between bulk hyperuniform systems. Using simulations of three distinct microscopic models, we demonstrate that hyperuniform interfaces are much smoother than equilibrium ones, with a universal reduction of height fluctuations at large scale. We derive a nonequilibrium interface equation from the field theory of the bulk order parameter, and predict a reduction in height fluctuations, $S_h(\boldsymbol{k}) \equiv \langle |h(\boldsymbol{k})|^2 \rangle \sim |\boldsymbol{k}|^{-1}$, in stark contrast to equilibrium capillary wave theory where $S_h(\boldsymbol{k}) \sim |\boldsymbol{k}|^{-2}$. Our results establish a new universality class for nonequilibrium interfaces, highlighting the fundamental role of suppressed bulk fluctuations in shaping interfacial dynamics far from equilibrium.

DOI: 10.1103/4b8v-4sbh

Interfaces and phase separations are fundamental phenomena driving the organization and dynamics of matter across scales, from soft condensed matter systems [1–4] to complex biological assemblies [5–9] or granular systems [10–14]. These processes regulate the behavior of systems where distinct phases coexist and interact, often leading to intricate interfacial dynamics [15] possibly shaping the geometry and controlling the physics of complex materials.

An equilibrium interface in a phase-separated system obeys capillary wave theory, with a Hamiltonian on large scales given by the excess area of the fluctuating interface [2]: $\mathcal{H}[h] = \gamma \boldsymbol{k}^2 h(\boldsymbol{k})/2$, where $h(\boldsymbol{k})$ is the Fourier transform of the interface height and γ the surface tension. By equipartition, the resulting static height correlations obey $S_h(\boldsymbol{k}) \equiv \langle |h(\boldsymbol{k})|^2 \rangle = k_B T |\boldsymbol{k}|^{-2}/\gamma$, with T the temperature, and diverges as $|\boldsymbol{k}|^{-2}$, a signature of massless Goldstone modes associated with broken continuous translational symmetry [16], in analogy with vibrational dynamics in crystals [17].

In contrast, nonequilibrium systems can exhibit qualitatively different interfacial behavior. While growing interfaces—such as those described by the Kardar-Parisi-Zhang equation—are well-studied examples [15], we focus instead on phase-separated systems with stable, nongrowing interfaces. In this case, the interface is driven by the nonequilibrium nature of the bulk phases that coexist. This can arise through external driving, such as boundary forcing [18–20] or shear [21,22], leading to phenomena including traveling waves [23], reduced surface tension [22,24], and interfacial instabilities [2].

Internally driven systems—such as active matter—offer further richness. These can sustain novel interfacial dynamics, including persistent traveling modes [25–27] and instabilities [28,29]. A vast majority of experimental and numerical investigations of stable interfaces in active and granular matter report $S_h(\boldsymbol{k}) \sim |\boldsymbol{k}|^{-2}$, in agreement with capillary wave theory, albeit with an effective surface tension and temperature [30–36] that account for the deviations from equilibrium. Recently, scalar active interfaces have been theoretically predicted to exhibit scaling laws distinct from equilibrium capillary behavior [37,38], with some numerical support [39].

Unlike many active systems, whose bulk and interfacial large-scale properties often resemble equilibrium behavior [40], non-equilibrium hyperuniform systems constitute a distinct class of matter characterized by anomalous fluctuations that defy equilibrium expectations [41,42]. Found in diverse contexts such as optimization problems in nature [43–45], driven colloids [46] or cosmology [47], these systems are of wide interest for their potential to form materials with novel physical properties [48,49]. Hyperuniformity is defined by the suppression of long-wavelength bulk density fluctuations $\delta\rho(\boldsymbol{k})$, with a vanishing bulk structure factor, $S_\rho(\boldsymbol{k}) \equiv \langle |\delta\rho(\boldsymbol{k})|^2 \rangle$, at small $\boldsymbol{k}$ [50]. Such behavior is forbidden in equilibrium systems with short-range interactions at finite temperature, where instead $S_\rho(\boldsymbol{k})$ converges to a finite value [41].

Here we study the statistical properties of the interface in phase coexistence between nonequilibrium hyperuniform systems. We construct and analyze three distinct microscopic models and observe that bulk hyperuniformity is inherited by the interface, which displays suppressed height fluctuations at large scale. We derive an interface equation that explains the observed behavior, which can be summarized as

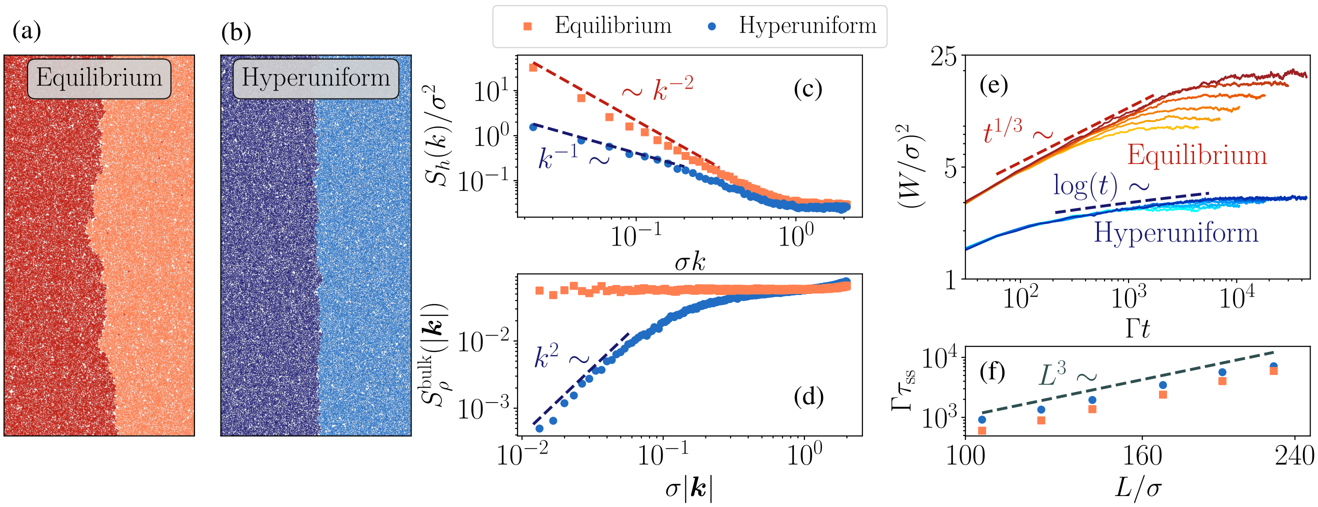

FIG. 1. Binary-mixture with active collisions. (a) Snapshot of a fully phase-separated AB mixture evolving under equilibrium Langevin dynamics with a square well potential interaction. The parameters are $T/U = -0.8$, $\sigma_U/\sigma = 1.6$, $m(\sigma\Gamma)^2/T = 0.075$, $N\pi\sigma^2/(4L_xL_y) = 0.55$, and $L_x = 1.81L_y$, where T is the kinetic energy of the system per particle. (b) Snapshot for the nonequilibrium system governed by Eqs. (2) and (3) with attraction. All parameters are identical to those in the equilibrium case without thermostat, and ΔE is chosen to match the kinetic energy of the equilibrium system. (c) Interface static height correlation functions for the two cases. (d) Radially averaged structure factors in the bulk. (e) Time evolution of W^2 for various system size for both models starting from a flat initial interface, averaged between 80 and 900 independent realizations. (f) Time to reach steady state τ_{ss} as a function of the short box length $L \equiv L_y$ for the systems in (e).

$t \to \infty$ and L large	W^2_{1d}	W^2_{2d}	$S_h(\boldsymbol{k})$
Equilibrium	$\sim L$	$\sim \log L$	$\sim\lvert\boldsymbol{k}\rvert^{-2}$
Hyperuniform	$\sim \log L$	const	$\sim\lvert\boldsymbol{k}\rvert^{-1}$

with $W^2(t) \equiv \langle[\langle h(\boldsymbol{r},t)\rangle - h(\boldsymbol{r},t)]^2\rangle$, the interface squared mean width. More generally, scale-free interfaces are characterized by two critical exponents which can be measured by starting from a flat interface at $t = 0$ in systems of linear size L [2]:

$$W^2(t) \sim \begin{cases} L^{2\chi} & \text{if } t \to \infty \\ t^{2\chi/z} & \text{if } L \to \infty \end{cases}, \qquad S_h(\boldsymbol{k}) \sim |\boldsymbol{k}|^{-d-2\chi}. \tag{1}$$

The dynamical exponent z is equivalently obtained from the relaxation time to the steady state, $\tau_{\mathrm{ss}}(L) \sim L^z$. Hyperuniform interfaces then display a suppression of height fluctuation from $|\boldsymbol{k}|^{-2}$ to $|\boldsymbol{k}|^{-1}$, and a reduction of the roughness exponent χ from $(2-d)/2$ to $(1-d)/2$.

We have numerically measured these reduced interface fluctuations for three distinct hyperuniform phase separated models with one-dimensional interfaces. A first mechanism to produce bulk hyperuniformity is to locally inject energy through nonequilibrium momentum-conserving collisions combined with global dissipation via viscous damping [42]. This provides a robust framework for the spontaneous emergence of bulk hyperuniformity in nonequilibrium fluids [51]. We consider a system of hard disks of mass m and diameter σ. When two particles i and j collide, they undergo a momentum-conserving collision accompanied by a constant energy increment $\Delta E > 0$:

$$\boldsymbol{v}'_i + \boldsymbol{v}'_j = \boldsymbol{v}_i + \boldsymbol{v}_j,$$
$$\frac{1}{2}m\left(\boldsymbol{v}'^2_i + \boldsymbol{v}'^2_j\right) = \frac{1}{2}m\left(\boldsymbol{v}^2_i + \boldsymbol{v}^2_j\right) + \Delta E, \tag{2}$$

where $\boldsymbol{v}'_i$ and $\boldsymbol{v}_i$ are the post- and precollisional velocities of the particle i, respectively. Particles are subject to a viscous damping Γ during their free flight:

$$\boldsymbol{v}(t) = \boldsymbol{v}(0)e^{-\Gamma t}. \tag{3}$$

In the model defined by Eqs. (2) and (3), phonons cannot propagate and the system becomes hyperuniform [52,53].

To induce phase separation and create a nonequilibrium interface, we introduce attractive interactions in addition to the non-equilibrium energy injecting collisions. We use a binary mixture with particles of types A and B, with attractive AA and BB interactions, but no attraction for AB. As in equilibrium, this results in a liquid-liquid phase separation at large enough attraction [54]. The attraction is modeled as a square potential with depth U and width σ_U. This model system can be regarded an idealization of a weakly cohesive quasi-2D vibrated granular gas. We will compare this system to an equilibrium one in which collisions are elastic, $\Delta E = 0$, and an uncorrelated Gaussian white noise with variance $2\Gamma T$ is added to thermalize the system.

We perform event-driven molecular dynamics simulations [55] of both equilibrium and non-equilibrium systems in a two-dimensional system of N particles in an elongated periodic box with $L_y < L_x$, using a 50:50 ratio of A and B particles. We operate away from the critical point, deep in the phase coexistence region. As shown in Figs. 1(a) and 1(b), the interface separating the two phases in the equilibrium system appears rougher than in the nonequilibrium system, despite the bulk phases in both cases being tuned to have the same average kinetic energy. This visual difference is quantified by the static height correlation S_h in Fig. 1(c). The equilibrium system exhibits the expected $|\boldsymbol{k}|^{-2}$ divergence, characteristic of thermal fluctuations. Instead, the interface separating the hyperuniform bulk fluids shows strongly suppressed fluctuations at large scale, compatible with a smaller $|\boldsymbol{k}|^{-1}$ divergence. We confirm in Fig. 1(d) that the bulk of each phase in the non-equilibrium phase separated system remains hyperuniform, even in the presence of attractive interactions. Figure 1(e) shows the time evolution of $W^2(t)$ in both models for different system sizes starting from a flat interface at $t = 0$. At equilibrium, as expected, we measure $W^2 \sim t^{2\chi/z}$ with $z = 3$ [2] for times before the saturation to a system size dependent plateau. For the hyperuniform system, however, the growth appears logarithmic as $\chi = 0$ and we cannot directly extract z from $W^2(t)$. Instead, we can use the equilibration time $\tau_{\mathrm{ss}}(L) \sim L^z$ as demonstrated in Fig. 1(f), and the results are compatible with $z = 3$.

To verify the universality of our findings, we now consider a second class of hyperuniform models: random organization models. These models originated from the study of sheared colloids and represent perhaps the simplest framework for generating hyperuniform states. We study two variants in two dimensions [17,46,56,57]. The system consists of N particles in a square box of side L with periodic boundary conditions, using again a 50:50 binary mixture with two types of particles. To introduce attractive interactions, we generalize the original dynamic rule as follows. At each discrete time step t, particle pairs (i, j) interact based on their pairwise distance r_{ij} via two interaction ranges σ_1 and $\sigma_2 > \sigma_1$. If $r_{ij} < \sigma_1$, particles undergo a repulsive displacement along the axis connecting the two centers, as in the original model. If $r_{ij} < \sigma_2$ and particles (i, j) belong to the same species, they undergo an attractive displacement along the axis connecting their centers. During a collision, the amplitude of the resulting displacement is drawn randomly from uniform distributions in the intervals $[0, \epsilon_1]$ and $[0, \epsilon_2]$, respectively.

In the conserved biased random organization model (CBRO), the displacement amplitudes are the same for the two interacting particles, so that the position of the center of mass is conserved [17,58]. This conservation law is the source of the bulk hyperuniformity. To assess the role of hyperuniformity on the interfacial dynamics, we also study the biased random organization model (BRO), where the displacement amplitudes of the two interacting particles are independent [59]. This second model displays equilibriumlike density fluctuations and is not hyperuniform.

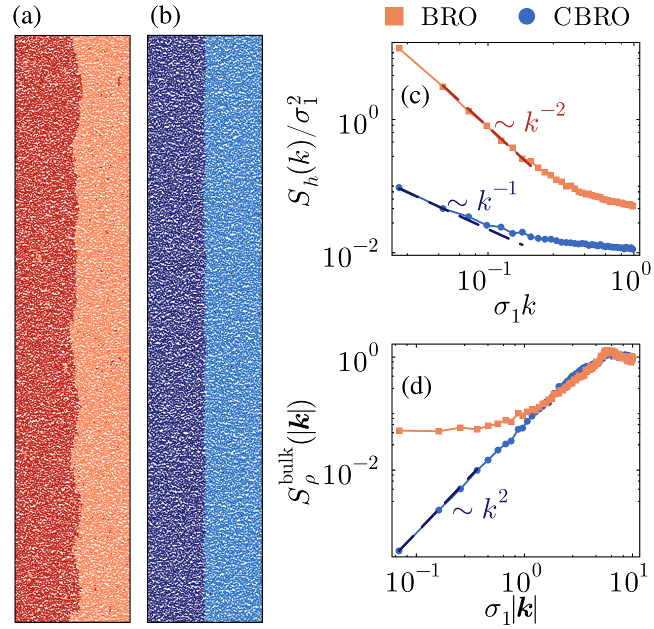

FIG. 2. Random organization models. (a),(b) Snapshots of a phase-separated mixtures evolving under BRO (a) and CBRO (b) dynamics. The parameters are $\sigma_2/\sigma_1 = 1.4$, $\epsilon_1/\sigma_1 = 0.5$, $\epsilon_2/\sigma_1 = 0.1$, $N = 5 \times 10^4$, $L = 256\sigma_1$. (c) Interface static height correlation functions. (d) Radially averaged structure factors in the bulk. Results are averaged over 20 independent realizations.

The snapshots in Figs. 2(a) and 2(b) show that the interface in the BRO model displays significantly more pronounced fluctuations compared to the CBRO model, where the interface appears nearly flat. The visual difference is quantitatively supported by the static height correlation $S_h(k)$ in Fig. 2(c), where the BRO model shows a $|\boldsymbol{k}|^{-2}$ scaling, consistent with equilibriumlike fluctuations, whereas the CBRO model displays a milder divergence, again compatible with $|\boldsymbol{k}|^{-1}$. Finally, Fig. 2(d) confirms the different nature of the density fluctuations in the bulk for the two models, even when attraction is present.

Our third model starts from Eqs. (2) and (3) in a monocomponent system instead of a bidisperse one, but promotes ΔE to a function of the time elapsed since the last collision, effectively linking activity to the local density. Specifically, after a collision, particles undergo a recharging period before they can again transfer significant energy in subsequent collisions, so that less energy is injected in regions where collisions are more frequent. This may trigger a phase separation without attractive forces [60], in analogy with motility induced phase separation in active matter [61]. Inspired by a model for vibrated granular materials, we choose [60]

$$\Delta E = 2\delta E_0 + \delta E\left(1 - e^{-\tau_i/\tau_r}\right)^\beta + \delta E\left(1 - e^{-\tau_j/\tau_r}\right)^\beta, \qquad (4)$$

with τ_i the time since the last collision of particle i, τ_r a charging time, and β controlling the form of the recharging

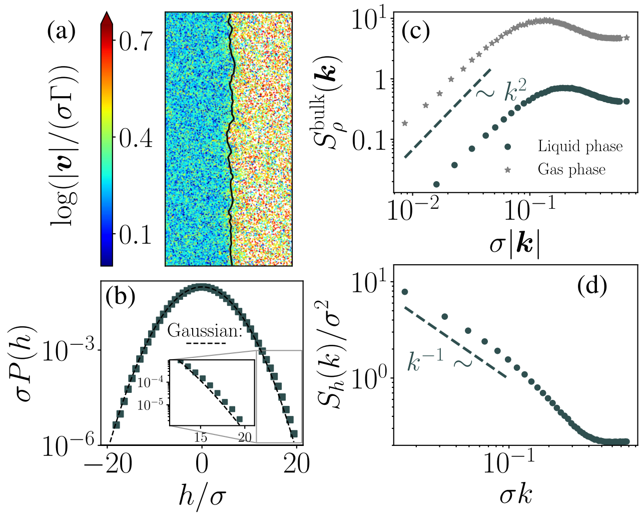

FIG. 3. Monocomponent system. (a) Snapshot with particles colored by velocity magnitude. (b) Probability distribution of height displacement h. The dashed line is a Gaussian fit. Inset: enlargement of the distribution tail to reveal the asymmetry of the distribution with measured skewness $\kappa_3 \simeq 0.045$ and excess kurtosis $\kappa_4 \simeq 0.031$ for this system size. (c) Structure factor of bulk coexisting liquid and gas phases. (d) Static height correlation. Parameters are $\delta E/\delta E_0 = 2\times 10^3$, $\beta = 10$, $\tau_r\Gamma = 0.2$, $\delta E_0/m(\sigma\Gamma)^2 = 10/36$, $L_x = 1.81 L_y = 383\sigma$, and $N\pi\sigma^2/(4L_xL_y) = 0.31$.

function. The energy injected in a collision varies between $2\delta E_0$ and $2\delta E_0 + 2\delta E$.

Figure 3(a) shows a typical snapshot of this model, with particles colored according to their velocities, demonstrating a phase separation between a dense phase with low kinetic energy, and a dilute phase with large velocities, consistent with underdamped nonequilibrium dynamics [11,62–64]. The difference in kinetic energy breaks the $h \to -h$ symmetry of the interface, as evidenced in Fig. 3(b) showing that the height density distribution $P(h)$ is biased towards the dilute phase. Figure 3(c) confirms that both phases maintain hyperuniformity. Figure 3(d) demonstrates our main result: the nonequilibrium interface exhibits suppressed fluctuations compatible with $S_h(\boldsymbol{k}) \sim |\boldsymbol{k}|^{-1}$.

To explain the observed universal suppression of interfacial fluctuations, $S_h(\boldsymbol{k}) \sim |\boldsymbol{k}|^{-1}$, in the three proposed models, we consider a coarse-grained equation for the dynamics of a conserved scalar order parameter $\phi(\boldsymbol{r}, t)$, representing either the local concentration (liquid-liquid) or the local density (liquid-gas). We generalize the linear model from Ref. [58] to account for phase separation in center-of-mass conserving systems:

$$\partial_t\phi = M\boldsymbol{\nabla}^2\frac{\delta F}{\delta\phi} + \sqrt{2D}\boldsymbol{\nabla}^2\xi,$$
$$\frac{\delta F}{\delta\phi} = -A\phi + A\phi^3 - \kappa\boldsymbol{\nabla}^2\phi, \tag{5}$$

where $F[\phi]$ is a free energy allowing for phase separation at $\phi = \pm 1$ [65], $\kappa > 0$ adds cost to gradients, and A, M, $D > 0$ are positive parameters and ξ is a random noise with zero mean and unit variance. Unlike equilibrium model B with noise term $\boldsymbol{\nabla}\cdot\boldsymbol{\eta}$ (conserving density but not center-of-mass), the noise $\boldsymbol{\nabla}^2\xi$ preserves the position of the center of mass [66]. Equation (5) can be derived from the Navier-Stokes equations governing the density and velocity fields of the monocomponent system described by Eqs. (2)–(4) (see Supplemental Material [67]). For the other two models, involving binary mixtures, we assume Eq. (5) still applies when the system is fully phase separated, thus neglecting interspecies diffusion. The binary mixture with damped velocity can also be described by an incompressible hydrodynamic equation instead of Eq. (5), from which all the results presented below can likewise be derived, as shown in the Supplemental Material [67]. In the linear regime, Eq. (5) correctly predicts bulk hyperuniformity, $S_\rho(\boldsymbol{k}) \propto |\boldsymbol{k}|^2$ [58].

To derive an equation for the interface, we make the standard ansatz [21]

$$\phi(\boldsymbol{r}, t) = f[r_\perp - h(\boldsymbol{r}_\parallel, t)], \tag{6}$$

where $r_\perp$ and $\boldsymbol{r}_\parallel$ are the axis orthogonal and parallel to the interface, respectively. The function $f(x)$ varies sharply at the interface position, $x = 0$. This ansatz projects the dynamics onto the interface h. By substituting Eq. (6) into Eq. (5) and retaining only leading-order contributions, we obtain (see Supplemental Material [67]) an equation for the interface dynamics:

$$\partial_t h(\boldsymbol{k}, t) = -\frac{\gamma_0 M}{2}|\boldsymbol{k}|^3 h(\boldsymbol{k}, t) + \sqrt{\frac{\gamma_0 D\boldsymbol{k}^2}{2\kappa}}\zeta(\boldsymbol{k}, t), \tag{7}$$

where ζ is a white noise with zero mean and unit variance, and $\gamma_0 \equiv \kappa\int f'(r_\perp)^2 dr_\perp$ the surface tension [2]. At equilibrium, the noise term in Eq. (7) would be proportional to $\sqrt{|\boldsymbol{k}|}\zeta$. This crucial difference in k factors arises from the difference between the equilibrium divergence noise and the nonequilibrium rather Laplacian noise. Equation (7) shows that nonequilibrium dynamics suppresses the height fluctuations leading to $\chi = (1-d)/2$ [instead of $\chi = (2-d)/2$ at equilibrium], so that

$$S_h(\boldsymbol{k}) = \frac{D}{2M\kappa}|\boldsymbol{k}|^{-1}. \tag{8}$$

This distinctive $|\boldsymbol{k}|^{-1}$ dependence, successfully observed across our three microscopic models, constitutes our main result. It shows that interface fluctuations between phase-separated hyperuniform phases are themselves strongly suppressed, thus leading to the concept of "hyperuniform interfaces" that are much flatter than their equilibrium counterparts [81]. For the dynamical exponent, we find $z = 3$, in agreement with Fig. 1.

Finally, we discuss the influence of additional nonequilibrium effects. In Eq. (5), nonequilibrium effects arise solely from the noise, while the deterministic part derives from a free energy. A nonequilibrium deterministic term in the order parameter equation would break the $h \to -h$ symmetry in the resulting interface equation [37]. The asymmetric distribution of h observed in Fig. 3 suggests the presence of such a term. The renormalization group analysis performed in the Supplemental Material [67] shows that this contribution is at most RG-marginal in $d = 1$, leading only to minor logarithmic corrections leaving the scaling behavior of S_h predicted by the linear theory in Eq. (7) unchanged. The marginality of the nonlinearity can also account for the weakness of the observed non-Gaussianity of $P(h)$ in Fig. 3(b).

In summary, we have identified a new universality class for interfacial behavior driven by bulk hyperuniformity. Our simulations of three physically distinct models, inspired by vibrated granular media, sheared colloidal suspensions, and active systems with trapping mechanisms, consistently revealed a strong suppression of interfacial fluctuations, a result supported by our theoretical analysis. This shared feature should lead to a finite interface width in two dimensions. This stands in contrast to the logarithmic divergence with system size observed at equilibrium, and lowers the lower critical dimension of the roughening transition by one. This finding provides a new example showing how hyperuniformity dramatically impacts the nature of fluctuations in nonequilibrium systems. For instance, it reduces the upper critical dimensions of $O(N)$ models [83], and enables phase transitions in low-dimensional systems with $N > 1$, bypassing the equilibrium lower critical dimension of 2 [84]. Likewise, it enables a breakdown of the Mermin-Wagner theorem in two-dimensional crystals, allowing true translational long-range order [17,52,85–89]. In all these cases, hyperuniformity efficiently suppresses the Goldstone modes arising from broken translational symmetry and decreases the lower critical dimension.

Because hyperuniform interfaces appear much smoother than equilibrium ones, this raises questions about the corresponding surface tension and possible physical consequences. Far from equilibrium, there exist multiple definitions of the surface tension. For example, using the capillary wave spectrum would directly lead to a diverging surface tension $\gamma \equiv \lim_{\boldsymbol{k}\to 0} T|\boldsymbol{k}|^{-2}/S_h(\boldsymbol{k}) \to \infty$, whereas this expression leads to a finite value at equilibrium. Instead, the nonequilibrium noise does not affect the surface tension γ_0 when using definitions based on Laplace pressure or the Buff-Kirkwood approach [90,91]. This contrasts with findings in active matter [28,92–94], where various novel effects are found from all definitions.

In future work, it would be interesting to extend our analysis to a broader range of nonequilibrium situations, such as chiral particles [95–98], cells [89,99], or other nonequilibrium systems [100–102]. A second avenue is to broaden the search for peculiar interfacial effects beyond nonequilibrium mechanisms. At equilibrium, long-range forces generically produce hyperuniformity [103], a peculiarity which also holds out of equilibrium [104,105]. How such interactions reshape interface thermodynamics, the existence of a surface tension and fluctuations, remains almost entirely uncharted [106].

Acknowledgments—We thank G. Foffi and F. Smallenburg for their invaluable help and insightful discussions throughout this project. We also greatly benefited from exchanges with L. Chaix, M. Grant, Y. Kuroda, A. Maitra, C. Nardini, L. Sarfati, J. Tailleur, and J. Toner. L. B. acknowledges the support of the French Agence Nationale de la Recherche (ANR), under Grants No. ANR-20-CE30-0031 (project THEMA) and No. ANR-24-CE30-0442 (project GLASSGO).

Data availability—The data that support the findings of this article are not publicly available upon publication because it is not technically feasible and/or the cost of preparing, depositing, and hosting the data would be prohibitive within the terms of this research project. The data are available from the authors upon reasonable request.

[1] R. A. Jones, *Soft Condensed Matter* (Oxford University Press, New York, 2002), Vol. 6.

[2] A. Onuki, *Phase Transition Dynamics* (Cambridge University Press, Cambridge, England, 2002).

[3] E. Zaccarelli, Colloidal gels: Equilibrium and non-equilibrium routes, J. Phys. Condens. Matter **19**, 323101 (2007).

[4] Y. H. Roos and S. Drusch, *Phase Transitions in Foods* (Academic Press, New York, 2015).

[5] A. A. Hyman, C. A. Weber, and F. Jülicher, Liquid-liquid phase separation in biology, Annu. Rev. Cell Dev. Biol. **30**, 39 (2014).

[6] W. M. Jacobs and D. Frenkel, Phase transitions in biological systems with many components, Biophys. J. **112**, 683 (2017).

[7] M. Sinhuber and N. T. Ouellette, Phase coexistence in insect swarms, Phys. Rev. Lett. **119**, 178003 (2017).

[8] S. Alberti, Phase separation in biology, Curr. Biol. **27**, R1097 (2017).

[9] G. W. Feigenson, Phase boundaries and biological membranes, Annu. Rev. Biophys. Biomol. Struct. **36**, 63 (2007).

[10] A. Plati, R. Maire, F. Boulogne, F. Restagno, F. Smallenburg, and G. Foffi, Self-assembly and non-equilibrium phase coexistence in a binary granular mixture, J. Chem. Phys. **163**, 054509 (2025).

[11] R. Maire, A. Plati, F. Smallenburg, and G. Foffi, Nonequilibrium coexistence between a fluid and a hotter or colder crystal of granular hard disks, J. Chem. Phys. **162**, 124901 (2025).

[12] J. P. Clewett, J. Wade, R. Bowley, S. Herminghaus, M. R. Swift, and M. G. Mazza, The minimization of mechanical work in vibrated granular matter, Sci. Rep. **6**, 28726 (2016).

[13] K. Roeller, J. P. D. Clewett, R. M. Bowley, S. Herminghaus, and M. R. Swift, Liquid-gas phase separation in confined vibrated dry granular matter, Phys. Rev. Lett. **107**, 048002 (2011).

[14] N. Mujica and R. Soto, Dynamics of noncohesive confined granular media, in *Recent Advances in Fluid Dynamics with Environmental Applications* (Springer, Cham, 2016), p. 445.

[15] A.-L. Barabási and H. E. Stanley, *Fractal Concepts in Surface Growth* (Cambridge University Press, Cambridge, England, 1995).

[16] R. Zia, R. Bausch, H. Janssen, and V. Dohm, Dynamics of an interface coupled to a diffusive bulk mode, Mod. Phys. Lett. B **02**, 961 (1988).

[17] L. Galliano, M. E. Cates, and L. Berthier, Two-dimensional crystals far from equilibrium, Phys. Rev. Lett. **131**, 047101 (2023).

[18] M. Grant and R. C. Desai, Fluctuating hydrodynamics and capillary waves, Phys. Rev. A **27**, 2577 (1983).

[19] N. Nakagawa and S.-I. Sasa, Liquid-gas transitions in steady heat conduction, Phys. Rev. Lett. **119**, 260602 (2017).

[20] S.-I. Sasa and N. Nakagawa, Non-equilibrium phase coexistence in boundary-driven diffusive systems, J. Stat. Phys. **192**, 1 (2025).

[21] A. J. Bray, A. Cavagna, and R. D. M. Travasso, Interface fluctuations, burgers equations, and coarsening under shear, Phys. Rev. E **65**, 016104 (2001).

[22] D. Derks, D. G. A. L. Aarts, D. Bonn, H. N. Lekkerkerker, and A. Imhof, Suppression of thermally excited capillary waves by shear flow, Phys. Rev. Lett. **97**, 038301 (2006).

[23] P. Barthelet and F. Charru, Benjamin-Feir and Eckhaus instabilities with Galilean invariance: The case of interfacial waves in viscous shear flows, Eur. J. Mech. B Fluids **17**, 1 (1998).

[24] C. Del Junco and S. Vaikuntanathan, Interface height fluctuations and surface tension of driven liquids with time-dependent dynamics, J. Chem. Phys. **150**, 094708 (2019).

[25] R. Adkins, I. Kolvin, Z. You, S. Witthaus, M. C. Marchetti, and Z. Dogic, Dynamics of active liquid interfaces, Science **377**, 768 (2022).

[26] L. Langford and A. K. Omar, Phase separation, capillarity, and odd-surface flows in chiral active matter, Phys. Rev. Lett. **134**, 068301 (2025).

[27] F. Raßhofer, S. Bauer, A. Ziepke, I. Maryshev, and E. Frey, Capillary wave formation in conserved active emulsions, arXiv:2505.20028.

[28] M. E. Cates and C. Nardini, Active phase separation: New phenomenology from non-equilibrium physics, Rep. Prog. Phys. **88**, 056601 (2025).

[29] L. Zhao, P. Gulati, F. Caballero, I. Kolvin, R. Adkins, M. C. Marchetti, and Z. Dogic, Asymmetric fluctuations and self-folding of active interfaces, Proc. Natl. Acad. Sci. U.S.A. **121**, e2410345121 (2024).

[30] L.-H. Luu, G. Castillo, N. Mujica, and R. Soto, Capillary like fluctuations of a solid-liquid interface in a noncohesive granular system, Phys. Rev. E **87**, 040202 (2013).

[31] L. Yao and R. L. Jack, Interfacial and density fluctuations in a lattice model of motility-induced phase separation, J. Chem. Phys. **162**, 114902(R) (2025).

[32] A. Wysocki, R. G. Winkler, and G. Gompper, Propagating interfaces in mixtures of active and passive Brownian particles, New J. Phys. **18**, 123030 (2016).

[33] L. Langford and A. K. Omar, Theory of capillary tension and interfacial dynamics of motility-induced phases, Phys. Rev. E **110**, 054604 (2024).

[34] A. Patch, D. M. Sussman, D. Yllanes, and M. C. Marchetti, Curvature-dependent tension and tangential flows at the interface of motility-induced phases, Soft Matter **14**, 7435 (2018).

[35] C. F. Lee, Interface stability, interface fluctuations, and the Gibbs-Thomson relationship in motility-induced phase separations, Soft Matter **13**, 376 (2017).

[36] S. Paliwal, V. Prymidis, L. Filion, and M. Dijkstra, Non-equilibrium surface tension of the vapour-liquid interface of active Lennard-Jones particles, J. Chem. Phys. **147**, 084902 (2017).

[37] M. Besse, G. Fausti, M. E. Cates, B. Delamotte, and C. Nardini, Interface roughening in nonequilibrium phase-separated systems, Phys. Rev. Lett. **130**, 187102 (2023).

[38] F. Caballero, A. Maitra, and C. Nardini, Interface dynamics of wet active systems, Phys. Rev. Lett. **134**, 087105 (2025).

[39] B. Krishan, Finite size scaling and universality classes of one-dimensional active matter interface, Europhys. Lett. **150**, 37003 (2025).

[40] É. Fodor, R. L. Jack, and M. E. Cates, Irreversibility and biased ensembles in active matter: Insights from stochastic thermodynamics, Annu. Rev. Condens. Matter Phys. **13**, 215 (2022).

[41] S. Torquato, Hyperuniform states of matter, Phys. Rep. **745**, 1 (2018).

[42] Y. Lei and R. Ni, Non-equilibrium dynamic hyperuniform states, J. Phys. Condens. Matter **37**, 023004 (2024).

[43] Y. Jiao, T. Lau, H. Hatzikirou, M. Meyer-Hermann, J. C. Corbo, and S. Torquato, Avian photoreceptor patterns represent a disordered hyperuniform solution to a multiscale packing problem, Phys. Rev. E **89**, 022721 (2014).

[44] S. Atkinson, G. Zhang, A. B. Hopkins, and S. Torquato, Critical slowing down and hyperuniformity on approach to jamming, Phys. Rev. E **94**, 012902 (2016).

[45] Z. Ge, The hidden order of Turing patterns in arid and semi-arid vegetation ecosystems, Proc. Natl. Acad. Sci. U.S.A. **120** (2023).

[46] E. Tjhung and L. Berthier, Hyperuniform density fluctuations and diverging dynamic correlations in periodically driven colloidal suspensions, Phys. Rev. Lett. **114**, 148301 (2015).

[47] O. H. E. Philcox and S. Torquato, Disordered heterogeneous universe: Galaxy distribution and clustering across length scales, Phys. Rev. X **13**, 011038 (2023).

[48] W. Man, M. Florescu, E. P. Williamson, Y. He, S. R. Hashemizad, B. Y. Leung, D. R. Liner, S. Torquato, P. M. Chaikin, and P. J. Steinhardt, Isotropic band gaps

and freeform waveguides observed in hyperuniform disordered photonic solids, Proc. Natl. Acad. Sci. U.S.A. **110**, 15886 (2013).

[49] W. Shi, Y. Jiao, and S. Torquato, Three-dimensional construction of hyperuniform, nonhyperuniform, and antihyperuniform disordered heterogeneous materials and their transport properties via spectral density functions, Phys. Rev. E **111**, 035310 (2025).

[50] S. Torquato and F. H. Stillinger, Local density fluctuations, hyperuniformity, and order metrics, Phys. Rev. E **68**, 041113 (2003).

[51] R. Maire and L. Chaix, Hyperuniformity and conservation laws in non-equilibrium systems, arXiv:2509.04242.

[52] R. Maire and A. Plati, Enhancing (quasi-)long-range order in a two-dimensional driven crystal, J. Chem. Phys. **161**, 054902 (2024).

[53] Q.-L. Lei and R. Ni, Hydrodynamics of random-organizing hyperuniform fluids, Proc. Natl. Acad. Sci. U.S.A. **116**, 22983 (2019).

[54] Y. Oku, K. Takae, and A. Ikeda, Phase separation kinetics of a symmetric binary mixture of glass-forming liquids, arXiv:2004.02103.

[55] F. Smallenburg, Efficient event-driven simulations of hard spheres, Eur. Phys. J. E **45**, 22 (2022).

[56] L. Corte, P. M. Chaikin, J. P. Gollub, and D. J. Pine, Random organization in periodically driven systems, Nat. Phys. **4**, 420 (2008).

[57] S. Anand, G. Zhang, and S. Martiniani, Emergent universal long-range structure in random-organizing systems, arXiv:2505.22933.

[58] D. Hexner and D. Levine, Noise, diffusion, and hyperuniformity, Phys. Rev. Lett. **118**, 020601 (2017).

[59] S. Wilken, R. E. Guerra, D. Levine, and P. M. Chaikin, Random close packing as a dynamical phase transition, Phys. Rev. Lett. **127**, 038002 (2021).

[60] D. Risso, R. Soto, and M. Guzmán, Effective two-dimensional model for granular matter with phase separation, Phys. Rev. E **98**, 022901 (2018).

[61] M. E. Cates and J. Tailleur, Motility-induced phase separation, Annu. Rev. Condens. Matter Phys. **6**, 219 (2015).

[62] L. Hecht, I. Dong, and B. Liebchen, Motility-induced coexistence of a hot liquid and a cold gas, Nat. Commun. **15**, 3206 (2024).

[63] S. Mandal, B. Liebchen, and H. Löwen, Motility-induced temperature difference in coexisting phases, Phys. Rev. Lett. **123**, 228001 (2019).

[64] L. Caprini, D. Breoni, A. Ldov, C. Scholz, and H. Löwen, Dynamical clustering and wetting phenomena in inertial active matter, Commun. Phys. **7**, 343 (2024).

[65] R. Evans, The nature of the liquid-vapour interface and other topics in the statistical mechanics of non-uniform, classical fluids, Adv. Phys. **28**, 143 (1979).

[66] F. De Luca, X. Ma, C. Nardini, and M. E. Cates, Hyperuniformity in phase ordering: The roles of activity, noise, and non-constant mobility, J. Phys. Condens. Matter **36**, 405101 (2024).

[67] See Supplemental Material at http://link.aps.org/supplemental/10.1103/4b8v-4sbh, which includes Refs. [68–80].

[68] A. J. Archer, D. J. Ratliff, A. M. Rucklidge, and P. Subramanian, Deriving phase field crystal theory from dynamical density functional theory: Consequences of the approximations, Phys. Rev. E **100**, 022140 (2019).

[69] A. J. Bray, Theory of phase-ordering kinetics, Adv. Phys. **43**, 357 (1994).

[70] F. Caballero, C. Nardini, F. van Wijland, and M. E. Cates, Strong coupling in conserved surface roughening: A new universality class?, Phys. Rev. Lett. **121**, 020601 (2018).

[71] J. R. Dorfman, H. van Beijeren, and T. R. Kirkpatrick, *Contemporary Kinetic Theory of Matter* (Cambridge University Press, Cambridge, England, 2021).

[72] V. Garzó, R. Brito, and R. Soto, Enskog kinetic theory for a model of a confined quasi-two-dimensional granular fluid, Phys. Rev. E **98**, 052904 (2018).

[73] V. Giovangigli, Kinetic derivation of diffuse-interface fluid models, Phys. Rev. E **102**, 012110 (2020).

[74] P. Illien, The Dean-Kkawasaki equation and stochastic density functional theory, Rep. Prog. Phys. **88**, 086601 (2025).

[75] H. Jacquin, B. Kim, K. Kawasaki, and F. Van Wijland, Brownian dynamics: From glassy to trivial, Phys. Rev. E **91**, 022130 (2015).

[76] H. K. Janssen, On critical exponents and the renormalization of the coupling constant in growth models with surface diffusion, Phys. Rev. Lett. **78**, 1082 (1997).

[77] M. Kardar, G. Parisi, and Y.-C. Zhang, Dynamic scaling of growing interfaces, Phys. Rev. Lett. **56**, 889 (1986).

[78] T. Sun, H. Guo, and M. Grant, Dynamics of driven interfaces with a conservation law, Phys. Rev. A **40**, 6763 (1989).

[79] M. te Vrugt, H. Löwen, and R. Wittkowski, Classical dynamical density functional theory: From fundamentals to applications, Adv. Phys. **69**, 121 (2020).

[80] J. Toner, *The Physics of Flocking: Birth, Death, and Flight in Active Matter* (Cambridge University Press, Cambridge, England, 2024).

[81] The reduced fluctuations could likewise be characterized through the related notion of local surface fluctuation introduced in Ref. [82].

[82] S. Torquato, Hyperuniformity and its generalizations, Phys. Rev. E **94**, 022122 (2016).

[83] S. Gao, H. Shang, H. Hu, Y.-Q. Ma, and Q.-L. Lei, Liquid-gas criticality of hyperuniform fluids, arXiv:2507.06023.

[84] H. Ikeda, Correlated noise and critical dimensions, Phys. Rev. E **108**, 064119 (2023).

[85] H. Ikeda, Harmonic chain far from equilibrium: Single-file diffusion, long-range order, and hyperuniformity, SciPost Phys. **17**, 103 (2024).

[86] C. Huang, L. Chen, and X. Xing, Alignment destabilizes crystal order in active systems, Phys. Rev. E **104**, 064605 (2021).

[87] S. Dey, A. Bhattacharya, and S. Karmakar, Enhanced long wavelength Mermin-Wagner-Hohenberg fluctuations in active crystals and glasses, Nat. Commun. **16**, 5498 (2025).

[88] Y. Kuroda, T. Kawasaki, and K. Miyazaki, Long-range translational order and hyperuniformity in two-dimensional chiral active crystal, Phys. Rev. Res. **7**, L012048 (2025).

[89] Y.-E. Keta and S. Henkes, Long-range order in two-dimensional systems with fluctuating active stresses, Soft Matter **21**, 5710 (2025).

[90] C. Braga, E. R. Smith, A. Nold, D. N. Sibley, and S. Kalliadasis, The pressure tensor across a liquid-vapour interface, J. Chem. Phys. **149**, 044705 (2018).

[91] P. R. ten Wolde and D. Frenkel, Computer simulation study of gas-liquid nucleation in a Lennard-Jones system, J. Chem. Phys. **109**, 9901 (1998).

[92] Y. Zhao, R. Zakine, A. Daerr, Y. Kafri, J. Tailleur, and F. van Wijland, Active Young-Dupré equation: How self-organized currents stabilize partial wetting, arXiv:2405.20651.

[93] R. Zakine, Y. Zhao, M. Knežević, A. Daerr, Y. Kafri, J. Tailleur, and F. van Wijland, Surface tensions between active fluids and solid interfaces: Bare vs dressed, Phys. Rev. Lett. **124**, 248003 (2020).

[94] L. Langford and A. K. Omar, The mechanics of nucleation and growth and the surface tensions of active matter, J. Chem. Phys. **163**, 064901 (2025).

[95] Y. Kuroda and K. Miyazaki, Microscopic theory for hyperuniformity in two-dimensional chiral active fluid, J. Stat. Mech. (2023) 103203.

[96] D. Kushwaha and S. Mishra, Chirality induced phase separation in active circle swimmers, Physica (Amsterdam) **677A**, 130897 (2025).

[97] J. Wang, Z. Sun, H. Chen, G. Wang, D. Chen, G. Chen, J. Shuai, M. Yang, Y. Jiao, and L. Liu, Active hyperuniform networks of chiral magnetic micro-robotic spinners, arXiv:2505.21820.

[98] Y. Kuroda, T. Kawasaki, and K. Miyazaki, Singular density correlations in chiral active fluids in three dimensions, Phys. Rev. E **112**, 045426 (2025).

[99] Z.-Q. Li, Q.-L. Lei, and Y.-Q. Ma, Fluidization and anomalous density fluctuations in 2D Voronoi cell tissues with pulsating activity, Proc. Natl. Acad. Sci. U.S.A. **122**, e2421518122 (2025).

[100] K. J. Wiese, Hyperuniformity in the manna model, conserved directed percolation and depinning, Phys. Rev. Lett. **133**, 067103 (2024).

[101] H.-H. Boltz and T. Ihle, Hyperuniformity in deterministic anti-aligning active matter, arXiv:2402.19451.

[102] R. Liu, M. Yang, and K. Chen, Hyperuniform mixing of binary active spinners, arXiv:2504.17197.

[103] T. Leblé, The two-dimensional one-component plasma is hyperuniform, arXiv:2104.05109.

[104] N. Oppenheimer, D. B. Stein, M. Y. B. Zion, and M. J. Shelley, Hyperuniformity and phase enrichment in vortex and rotor assemblies, Nat. Commun. **13**, 804 (2022).

[105] V. Yashunsky, D. J. Pearce, G. Ariel, and A. Be'er, Topological defects in multi-layered swarming bacteria, Soft Matter **20**, 4237 (2024).

[106] K. R Mecke and S. Dietrich, Effective Hamiltonian for liquid-vapor interfaces, Phys. Rev. E **59**, 6766 (1999).